AGU PUBLICATIONS

JGR

Journal of Geophysical Research: Atmospheres

RESEARCH ARTICLE
10.1002/2015JD024316

Key Points:
- Arctic winter cloud cover causes changes in summer sea ice thickness and area
- Data from the last three decades show that clouds impose regional and large-scale changes on sea ice
- The 2007 sea ice minimum can be explained in part by anomalous winter cloud forcing

Correspondence to:
A. Letterly,
aaron.letterly@ssec.wisc.edu

Citation:
Letterly, A., J. Key, and Y. Liu (2016), The influence of winter cloud on summer sea ice in the Arctic, 1983–2013, *J. Geophys. Res. Atmos.*, *121*, doi:10.1002/2015JD024316.

Received 19 OCT 2015
Accepted 15 FEB 2016
Accepted article online 18 FEB 2016

The influence of winter cloud on summer sea ice in the Arctic, 1983–2013

Aaron Letterly[1], Jeffrey Key[2], and Yinghui Liu[1]

[1]Cooperative Institute of Meteorological Satellite Studies, University of Wisconsin-Madison, Madison, Wisconsin, USA, [2]NOAA/NESDIS, Madison, Wisconsin, USA

Abstract Arctic sea ice extent has declined dramatically over the last two decades, with the fastest decrease and greatest variability in the Beaufort, Chukchi, and East Siberian Seas. Thinner ice in these areas is more susceptible to changes in cloud cover, heat and moisture advection, and surface winds. Using two climate reanalyses and satellite data, it is shown that increased wintertime surface cloud forcing contributed to the 2007 summer sea ice minimum. An analysis over the period 1983–2013 reveals that reanalysis cloud forcing anomalies in the East Siberian and Kara Seas precondition the ice pack and, as a result, explain 25% of the variance in late summer sea ice concentration. This finding was supported by Moderate Resolution Imaging Spectroradiometer cloud cover anomalies, which explain up to 45% of the variance in sea ice concentration. Results suggest that winter cloud forcing anomalies in this area have predictive capabilities for summer sea ice anomalies across much of the central and Eurasian Arctic.

1. Introduction

Over the last two decades, the Arctic has experienced a significant decline in sea ice extent. The decreasing ice extent corresponds to a warming of the Arctic at more than twice the global average, known as Arctic amplification. Though Arctic amplification is anticipated to cause warming through the year 2100 [*Holland and Bitz*, 2003; *Zhang and Walsh*, 2006; *Overland and Wang*, 2013] with a continuing decrease in sea ice extent, interannual variation in Arctic sea ice extent is difficult to predict.

Arctic sea ice extent is forced by a number of feedback mechanisms, with ice-albedo and cloud-radiation feedbacks contributing significantly toward sea ice growth and melt [*Serreze and Francis*, 2006; *Curry et al*., 1996]. Large-scale atmospheric variability has also been shown to contribute to the sea ice decline, particularly changes in such modes of circulation as the Arctic Dipole Anomaly pattern [*Overland et al*., 2012; *Wang et al*., 2009] and the Northern Annular Mode [*Deser and Teng*, 2008; *Ogi and Rigor*, 2013].

The effect of Arctic clouds on the surface energy budget is substantial [*Curry et al*., 1996; *Intrieri et al*., 2002; *Liu et al*., 2008; *Tjernström et al*., 2008]. Arctic clouds warm the surface except during part of the summer [*Intrieri et al*., 2002; *Stone*, 1997; *Schweiger and Key*, 1994]. Seasonal changes in Arctic cloud amount have been observed and will also affect the surface energy budget [*Liu et al*., 2007, 2008, 2009; *Schweiger*, 2004; *Wang and Key*, 2003, 2005b].

The effect of sea ice changes on cloud cover is well documented [*Vavrus et al*., 2009, 2011; *Schweiger et al*., 2008a; *Cuzzone and Vavrus*, 2011; *Kay and Gettelman*, 2009; *Palm et al*., 2010; *Liu et al*., 2012], but the capability of cloud cover changes to influence sea ice is less studied. *Pithan and Mauritsen* [2013] examined a variety of climate models to determine the effect of clouds on surface temperature. Their results showed that climate models gave different answers regarding the net warming or cooling effect of clouds on the Arctic surface.

Also uncertain is the effect of downwelling shortwave anomalies on sea ice. *Kay et al*. [2008] used climate reanalyses to determine that decreases in summer cloud cover increased the downwelling shortwave radiation at the surface and contributed to the 2007 ice extent minimum, citing 2.4 K of warming to the ocean by cloud and radiation anomalies alone. In contrast, *Nussbaumer and Pinker* [2012] found that ice areas receiving the largest amounts of downwelling shortwave radiation from January to June do not correspond to negative sea ice concentration anomalies. *Schweiger et al*. [2008b] also found that the downwelling shortwave flux and negative cloud anomalies over the summer months had no appreciable contribution to the sea ice extent minimum. *Kauker et al*. [2009] discussed the minor impacts of cloud reductions in summer on ice extent but related the 2007 minimum primarily to wind conditions in May and June, surface temperature in September,

and ice thickness in March. *Perovich et al*. [2008] assigned the primary cause of enhanced ice loss in the Beaufort Sea during the summer of 2007 to be enhanced heating of the upper ocean, though cloud effects on this heating were not explicitly mentioned.

Many of these studies are devoted to the radiative effects of spring or summer clouds, seasons in which downwelling shortwave radiation can be the largest contributor to the surface energy budget. During most of the year, the downwelling longwave flux dominates the surface radiation budget. *Stone et al*. [2005] found that a 5% increase in winter cloud cover during February at Barrow, Alaska, led to increased surface temperatures of 1.4°C, on average, over a 33 year period. Over sea ice, *Kapsch et al*. [2013] and *Graversen et al*. [2011] showed that increased downwelling longwave radiation caused by springtime cloud cover corresponds to years with negative sea ice anomalies in the summer. Similarly, *Park et al*. [2015] show that summers with anomalously small sea ice area are preceded by winters with above-average downward longwave radiation, particularly over the Eurasian portion of the Arctic Ocean. They attribute this primarily to anomalously strong moisture flux intrusions into the Arctic. The influence of wintertime cloud cover on surface radiation anomalies has been explored at length [*Curry et al*., 1996], but fewer studies have addressed the seasonally lagged contribution of winter clouds on summertime sea ice. *Francis et al*. [2009] explored Arctic atmospheric "memory" between autumn weather and summer sea ice. This system memory is further explored by *Liu and Key*'s [2014] use of climate reanalyses and satellite data to determine that below-average cloud cover in the winter of 2013 contributed to the summertime sea ice area rebound from the record low of 2012.

This study extends the work of *Liu and Key* [2014] by examining the role of wintertime cloud anomalies on summertime sea ice concentration over three decades. Cloud radiative forcing from two climate reanalysis products, a satellite cloud cover product, and sea ice concentration from passive microwave satellite data are the primary data sets employed. The validity of using reanalysis results is supported by comparison to passive and active remote sensing products. The winter preceding the 2007 record (at the time) sea ice minimum is used as a case study to examine the lagged effect of cloud forcing on rapid sea ice change. Arctic clouds are analyzed in a climatological context by determining long-term radiative contributions and relationships with ice concentration over the satellite record. Though large-scale atmospheric heat transport and ice dynamics undoubtedly contributed to the significant decrease in sea ice extent over this time period, this study does not attempt to address them. Instead, it focuses on the increases and decreases in winter cloud cover that, year after year, may precondition the marginal sea ice zones for rapid changes in ice area. Understanding the relationship between wintertime clouds and summertime ice will aid in determining whether clouds play a significant role in abrupt year-to-year ice concentration changes, the long-term hemispheric sea ice decline, or both.

2. Data and Methods

The geophysical variables of primary interest are cloud radiative effect, or "forcing," and sea ice concentration. Cloud forcing refers to the difference in the net radiation flux between cloudy and clear-sky conditions. In winter, positive cloud radiative forcing creates a less negative surface radiation budget and inhibits ice formation, whereas a negative forcing leads to greater ice growth. Cloud radiative forcing is the integrated partial derivative of net radiative flux with respect to cloud fraction:

$$\mathrm{CS_S} = \int_0^{A_c} \frac{\partial S_S}{\partial a}\,\mathrm{d}a = S_S(A_c) - S_S(0) \tag{1}$$

$$\mathrm{CF_S} = \int_0^{A_c} \frac{\partial F_S}{\partial a}\,\mathrm{d}a = F_s(A_c) - F_S(0) \tag{2}$$

$$\mathrm{CNET_S} = \mathrm{CS_S} + \mathrm{CF_S} \tag{3}$$

where $\mathrm{CS_S}$, $\mathrm{CF_S}$, and $\mathrm{CNET_S}$ are the shortwave, longwave, and net cloud forcing at the surface, A_c is the total cloud amount, a is the cloud fraction, and S_S and F_S are the net shortwave and longwave fluxes at the surface.

To represent the total seasonal cloud forcing anomaly, the monthly anomaly fields were summed over four winter months from November to February into a single value, hereafter referred to as the "cumulative cloud forcing." There is no downwelling shortwave radiation during the winter months at very high latitudes (the "polar night") and little at the lower latitudes of the Arctic. Nevertheless, the shortwave cloud forcing is included in the cumulative cloud forcing.

The primary data sets used in this study include satellite-derived sea ice concentration and cloud radiative forcing from climate reanalyses. The daily sea ice concentration product is based on the National Aeronautics and Space Administration (NASA) "Team" algorithm [*Cavalieri et al*., 1996; *Maslanik and Stroeve*, 1999], which uses passive microwave brightness temperatures from the Defense Meteorological Satellite Program Special Sensor Microwave Imager (SSMI) and the Special Sensor Microwave Imager/Sounder (SSMIS). The Cloud-Aerosol Lidar and Infrared Pathfinder Satellite Observation (CALIPSO) [*Winker et al*., 2003] satellite cloud cover field is compared to the spatial patterns of cloud cover seen in Moderate Resolution Imaging Spectroradiometer (MODIS) products.

Surface radiation and cloud cover are obtained from the NASA Modern-Era Retrospective Analysis for Research and Applications (MERRA) [*Rienecker et al*., 2011] and the European Centre for Medium-Range Weather Forecasts (ECMWF) ERA-Interim Reanalysis [*Dee et al*., 2011]. MERRA covers the modern satellite era, 1979 to present, at ⅔° longitude by ½° latitude. ERA-Interim, the latest ECMWF global atmospheric reanalysis, covers a similar time period. In this study, monthly data are used though daily and hourly data are available.

These reanalyses were chosen because they yield similar results and have been shown to be in agreement with satellite-derived Arctic clouds, particularly MERRA [*Liu and Key*, 2014]. Other investigators have also found them to be adequate for studies involving Arctic surface radiative fluxes. For example, in their analysis of seven reanalysis products over the Arctic, *Lindsay et al*. [2014] found that three stood out as being more consistent with observations, including MERRA and ERA-Interim, and that wintertime downwelling longwave bias was smallest for MERRA. *Zib et al*. [2012] found that ERA-Interim performed well with regard to surface downwelling fluxes over two Arctic sites. Similarly, *Cox et al*. [2014] found that ERA-Interim performed well for shortwave and longwave surface fluxes over Summit, Greenland, but encountered some difficulty simulating thick clouds during winter.

Other data sets employed in this study include cloud cover from the NASA Moderate Resolution Imaging Spectroradiometer (MODIS) on the Aqua and Terra satellites, monthly average sea ice thickness from the advanced very high resolution radiometer (AVHRR) Polar Pathfinder-Extended (APP-x) product [*Key and Wang*, 2015; *Wang et al*., 2010], and sea ice motion vectors from the original AVHRR Polar Pathfinder (APP) product, which is based on AVHRR and passive microwave satellite data as well as drifting ice buoys [*Fowler et al*., 2013]. All products were remapped to the same 25 km projection (Equal-Area Scalable Earth (EASE)-Grid).

The approximate effect of the cloud forcing anomaly on changes in ice thickness was estimated using the simple model of *Thorndike* [1992]. Changes in ice thickness are related to surface net radiation as

$$\Delta h = \frac{t}{\rho L}[F_S + S_S + F_W] \tag{4}$$

where t is the length of the time period, ρ is the sea ice density (917 kg m^{-3}), L is the latent heat of fusion of ice (333.4 kJ kg^{-1}), F_S is the surface net longwave radiation, S_S is the surface net shortwave radiation, and F_W is the conductive heat flux at the ice-ocean interface. This equation is similar to that of *Eisenman et al*. [2007]. Since turbulent surface fluxes (sensible and latent heat) and the conductive flux are much smaller than the radiative fluxes [*Thorndike*, 1992; *Eisenman et al*., 2007], and because the focus of this study is on the radiative effect of clouds, they are neglected in this model. Nevertheless, ignoring turbulent and conductive heat fluxes introduces some error. For example, the conductive heat flux is likely to decrease with increased ice thickness, so ice growth will be less for thicker ice with equal cloud radiative forcing. Given that the conductive heat flux, surface emissivity, and albedo are all functions of snow depth, the uncertainty in the snow depth would produce additional error in sea ice growth estimates. In this study, however, we are interested only in demonstrating the sensitivity of ice thickness to surface radiation.

To determine the effects of a cloud forcing anomaly on ice growth, equation (4) can be rearranged using 1–3 as

$$\Delta h = \frac{t}{\rho L}[\mathrm{CNET}_S + F_{\mathrm{net}}(0)] \tag{5}$$

where $F_{\mathrm{net}}(0)$ is the surface net radiation for clear sky (only) and CNET_S is the surface net cloud radiative forcing anomaly. Anomalies are defined as departures from the 1983–2013 detrended monthly means. Using the above method, 1 W m^{-2} of negative cloud forcing anomaly per month would theoretically grow 0.85 cm of sea ice.

3. Winter 2007 Cloud Amount and Radiative Effect

September 2007 marked the second lowest Arctic sea ice extent since measurements began in 1979. Other studies have examined the historic minimum and claim that the decreased sea ice was a result of decreased summer cloud cover [*Kay et al*., 2008], increased heating by the ocean [*Perovich et al*., 2008], wind conditions, and already-reduced ice thicknesses [*Kauker et al*., 2009]. In this section we show that preconditioning for extreme ice loss began earlier than the 2007 spring in that positive cloud anomalies during the previous winter over the East Siberian Sea led to a decrease in the rate of sea ice growth. The resulting somewhat thinner ice was then advected toward the central Arctic, where it melted as surface temperatures increased in the spring and summer. By September, the ice initially thinned by increased winter cloud forcing had completely melted, explaining a significant amount of the negative sea ice anomaly. In contrast, *Liu and Key* [2014] demonstrated physical connections between significant cloud anomalies and dramatic sea ice change for the opposite case, where significantly below normal winter cloud cover led to increased ice growth which in turn contributed to a large rebound in 2013 September ice extent relative to the 2012 minimum.

In the winter preceding the sea ice minimum of September 2007, MERRA and ERA-Interim showed significant positive cloud forcing anomalies that resulted in increased downwelling longwave radiation over the East Siberian Sea, Laptev Sea, and other regions of the Alaskan and Siberian coastline (Figure 1). Four months of increased cloud cover in these regions were an important factor in keeping sea ice from reaching typical thicknesses, which may have ultimately contributed to a sea ice record minimum in September. The magnitude and spatial patterns of the positive cloud forcing anomaly were further verified with cloud cover anomalies from MODIS and CALIPSO data in Figure 1.

Multiple data sources indicated substantial anomalies in cloud cover and cloud radiative forcing over the winter of 2006–2007. CALIPSO, using monthly mean cloud forcing from 2006 to 2013 as a baseline, determined that over the majority of the East Siberian and Laptev Seas there were positive anomalies of approximately 20% in February 2007. Figure 1 shows that spatial patterns of positive cloud anomaly are supported by MODIS Aqua and Terra, where cloud amount over these areas was greater than two standard deviations from the 2002–2012 monthly mean.

Sea ice loss resulting from the October 2006 to February 2007 positive cloud forcing anomaly given in Figure 2 (left) is based on cloud radiative forcing from MERRA and the *Thorndike* [1992] model. Anomalies of up to 30 W m^{-2} occur throughout the East Siberian, Chukchi, and Laptev Seas, the same areas with greatly decreased ice concentration the following summer. Using the method from equation (5), these cloud forcing anomalies account for a decrease in ice thickness of 25 cm (Figure 2). However, regions of increased cloud forcing in Figure 2 (left) do not match exactly with the areas of decreased ice concentration in September. The differences in spatial pattern may be explained by ice drift.

After calculating the changes in thickness from the cloud forcing anomalies, satellite-derived sea ice motion vectors were used to move the ice thickness anomaly field from March to August. The final advected ice thickness changes are shown in Figure 2. The thinned ice resulting from increased cloud forcing corresponds spatially with anomalously low September sea ice concentration over the East Siberian and Laptev Seas, as shown in Figure 2 (right). This is the same methodology used by *Liu and Key* [2014] with a similar result for an opposite case (i.e., negative winter cloud anomaly and positive summer sea ice anomaly). Of course, cloud cover changes over the summer months may have contributed to the extensive ice loss in 2007 as well.

4. Climatological Relationship Between Winter Clouds and Summer Sea Ice

The 2007 case described above, and the 2013 case presented by *Liu and Key* [2014], demonstrates the substantial influence that winter clouds may have on summer sea ice. Does this relationship exist in a climatological sense? How frequently have significant wintertime cloud forcing anomalies influenced summertime sea ice anomalies over the last three decades?

In this section, cloud forcing anomalies from reanalysis data are compared with passive microwave ice concentrations from 1983 to 2013. Removing the long-term trends from both time series is necessary to interpret clouds' year-to-year effect on sea ice. To detrend the data, a linear regression equation was generated at each location (pixel) for both ice concentration and cloud forcing using the entire time period. Using a higher-order regression (i.e., third order) to remove the trend had almost no effect on the results, with a change in the

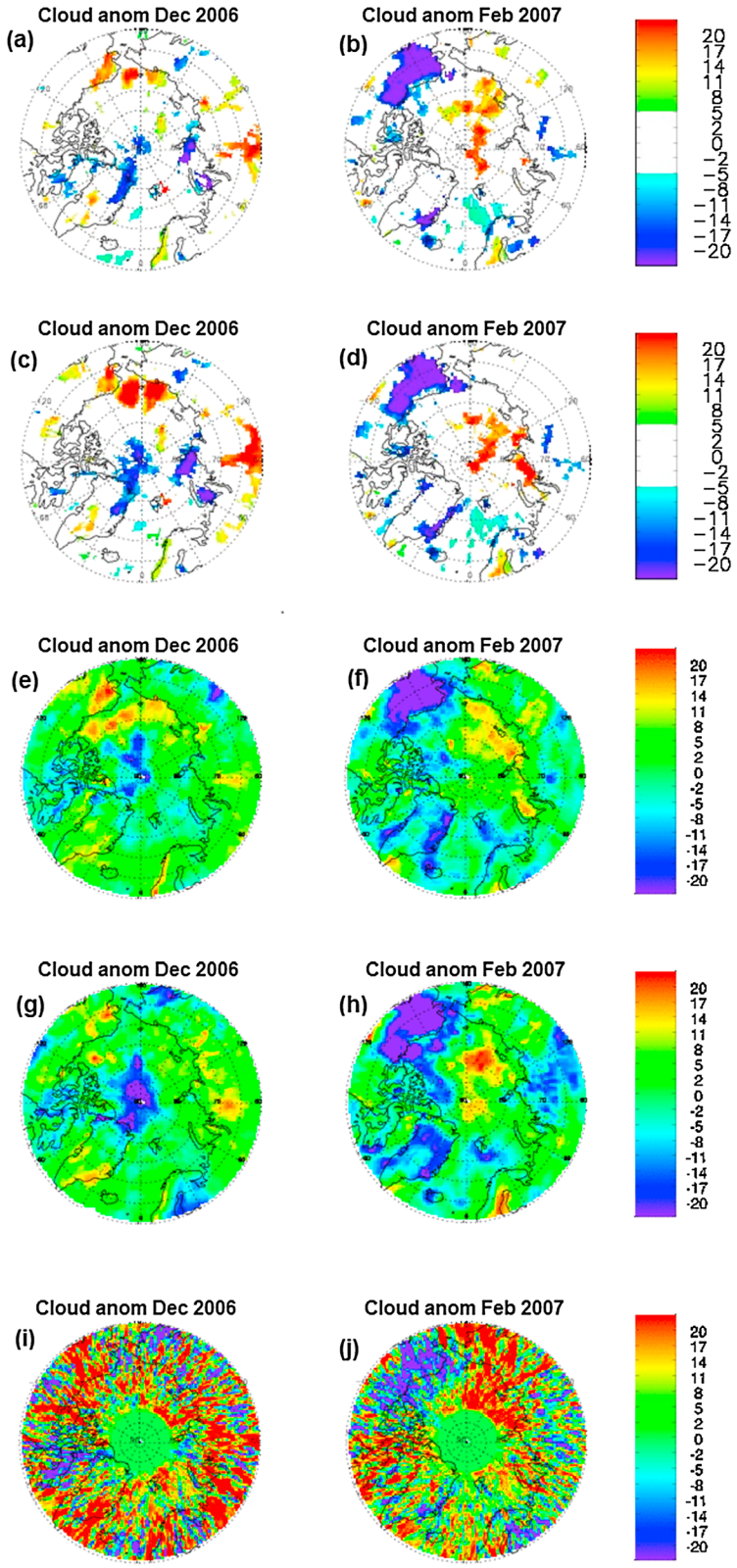

Figure 1. (a, c, e, g, and i) Cloud cover anomalies (%) in December 2006 for Aqua MODIS (Figure 1a), Terra MODIS (Figure 1c), the MERRA (Figure 1e), the ERA-Interim (Figure 1g), and CALIPSO (Figure 1i). (b, d, f, h, and j) February 2007 cloud cover anomaly (%) for Aqua MODIS (Figure 1b), Terra MODIS (Figure 1d), MERRA (Figure 1f), ERA-Interim (Figure 1h), and CALIPSO (Figure 1j).

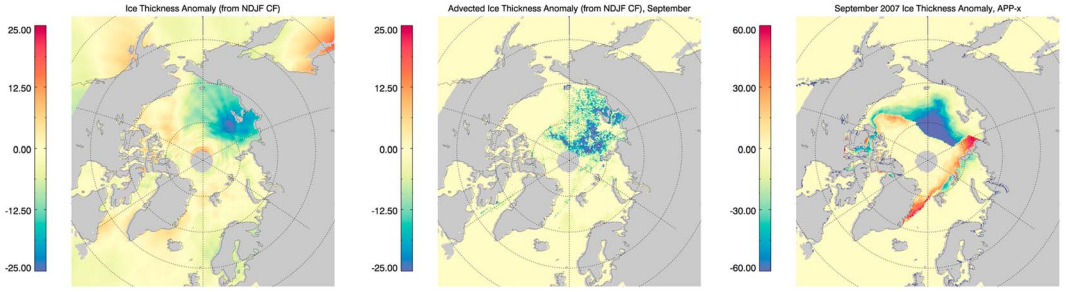

Figure 2. (left) Changes in ice thickness (cm) estimated from MERRA net cloud radiative forcing anomalies from November 2006 to February 2007. (middle) Ice thickness distribution at the beginning of September due to ice drift. (right) Detrended sea ice thickness anomalies for September 2007 from APP-x.

correlation coefficient only in the third decimal place. For any given month and location, the anomaly was calculated by taking the difference between the actual value and the predicted value from the regression equation. Figure 3 compares the 4 month cumulative cloud forcing anomalies with ice concentration anomalies over the East Siberian Sea. At this latitude, shortwave cloud forcing anomalies over the winter months contributed less than 0.5 W m^{-2} over a 4 month period. The data show an inverse relationship between cloud forcing and ice concentration anomalies for 77% of years from 1983 to 2013, where low (high) ice summers occur after winters with high (low) cloud forcing anomalies. The linear correlation between these two variables is −0.50.

Similarly, Terra MODIS cloud cover anomaly during winter from 2001 to 2013 showed a significant anticorrelation (−0.67) with September sea ice concentration anomaly. From November to February, increased cloud cover results in a more positive cloud forcing anomaly and decreased cloud results in a more negative cloud forcing anomaly, meaning that the cloud cover observations from MODIS should have the same sign of the reanalysis cloud forcing anomaly for the corresponding years. The Terra MODIS cloud cover anomalies do, in fact, have the same sign as MERRA for 10 out of the 13 years studied (77%). For ERA-Interim and MODIS, only 6 out of the 13 (46%) years had the same sign. The MERRA anomalies and Terra MODIS anomalies are compared in Figure 5. This comparison is important because differences in the two reanalyses could, in theory, lead to different conclusions. Using MODIS cloud cover as verification increases our confidence in the results.

Pixel-by-pixel correlations between the winter (November–February) cloud cover anomaly and the September sea ice concentration anomaly show the lagged connection between the two variables over the 31 year time series (Figures 4 and 5). Over the East Siberian and Kara Seas, inverse relationships greater than |0.5| indicate that winter clouds pose a strong control on summer sea ice, though this is a statistical relationship that does not prove causality. Isolated regions of the central Arctic Ocean exhibit direct relationships between the cloud forcing and sea ice concentration anomalies, but the physical connection is unclear given the typically thick

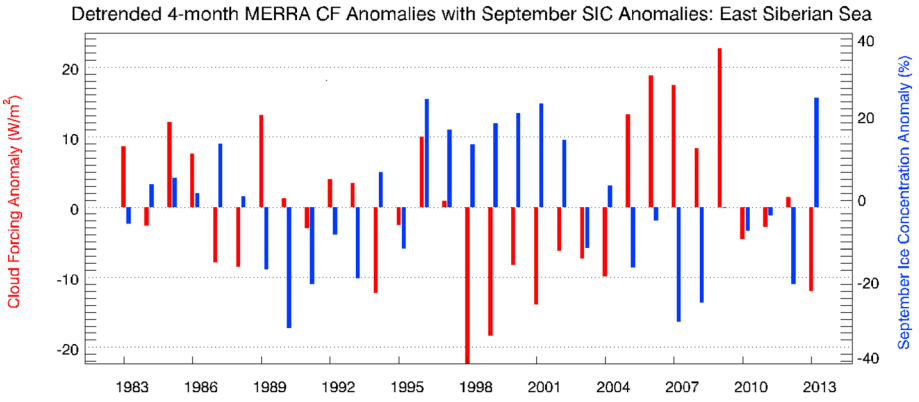

Figure 3. Time series comparing cumulative November–February all-wave cloud forcing anomalies (red) with September ice concentration anomaly (blue) over the East Siberian Sea region. Both variables are detrended.

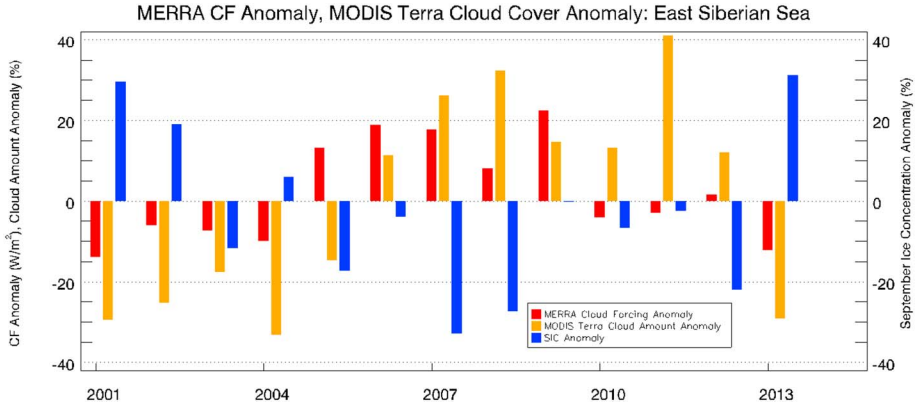

Figure 4. Time series comparing cumulative MERRA November–February all-wave cloud forcing anomalies (red) with MODIS cloud cover anomaly (orange) against September ice concentration anomaly (blue) over the East Siberian Sea region.

multiyear ice present in those areas. The same analysis was performed with ERA-Interim, which showed direct relationships between winter cloud and summer sea ice in the central Arctic and East Siberian Sea. This result may be due to the inability of ERA-Interim to simulate instances of heavy downwelling longwave from optically thick clouds during the wintertime [*Cox et al.*, 2014] Regardless, when the ERA-Interim and MERRA results were limited to relationships significant at the 0.9 confidence interval, positive correlations in the East Siberian Sea and central Arctic decreased dramatically. The remaining statistically significant correlations in the region of interest are largely negative and may be compared in Figure 5.

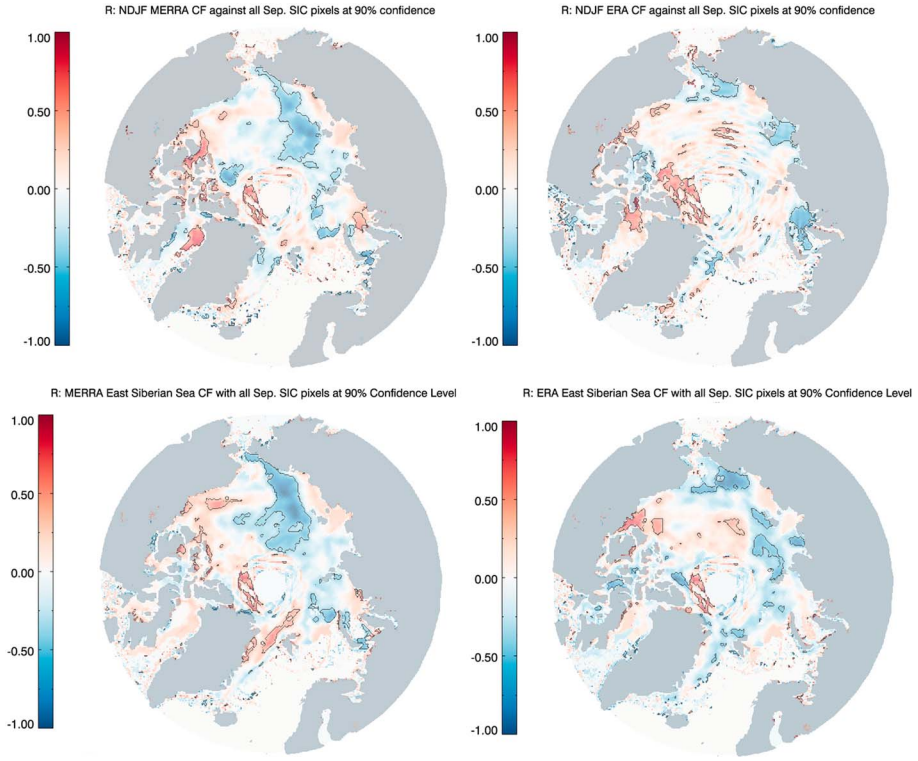

Figure 5. (top row) Point-by-point mapping of correlations between the cumulative November–February net cloud radiative forcing anomaly and the SSMIS September sea ice concentration anomaly the following summer for MERRA (left) and ERA-Interim (right). Both variables were detrended. Contours are drawn around correlations at the 0.9 confidence interval. (bottom row) Correlations between the cloud forcing anomaly in the East Siberian Sea region (only) and September ice concentration anomaly at all points in the Arctic the following summer for MERRA (left) and ERA-Interim (right), from 1983 to 2013.

The East Siberian Sea is only a portion of the Arctic Ocean, yet its location relative to large-scale atmospheric circulations allows changes in its ice cover to influence sea ice on a much larger scale. The Beaufort Gyre is a wind-driven, anticyclonic circulation that advects ice westward from the Beaufort Sea across the Chukchi Sea and then northward from the East Siberian Sea. *Liu and Key* [2014] showed that the Beaufort Gyre caused significant sea ice drift that redistributed first-year ice from January to September 2013. Over the satellite record, winter cloud forcing anomalies in the East Siberian Sea are inversely correlated with September ice concentration anomalies throughout the central and Siberian Arctic (Figures 4 and 5), forced by westward and northward ice drift from the Beaufort Gyre. Significant inverse correlations, seen in both MERRA and ERA-Interim, between cloud forcing in the East Siberian Sea and ice concentration across much of the central Arctic point out the strong predictive capacity of these regions on basin-wide ice extent and area. Other processes, such as ocean heating, freshwater flux, and solar insolation may affect this correlation. Nevertheless, the statistical link discussed here adds significance to cloud forcing anomalies in the East Siberian Sea region.

5. Discussion

Clouds represent only one of the processes governing changes in sea ice. Overall, the radiative effect of clouds is smaller than other climate processes in the Arctic such as the ice-albedo feedback [*Pithan and Mauritsen*, 2013]. However, this analysis has shown that reanalysis winter cloud forcing anomalies account for approximately 25% of the variance in East Siberian Sea and Kara Sea ice concentration over the satellite data record. Over a shorter time period, from 2001 to 2013, the MODIS winter cloud cover anomaly can explain 45% of the variance in summer sea ice concentration for the same region. This lagged dependence of summer ice concentration on winter cloud demonstrates that the memory of marginal sea ice regions can be anywhere from 7 to 10 months. The strength of the relationship between winter cloud and summer ice is founded on the amount of downwelling longwave radiation incident on the ice surface and therefore may depend on the types of clouds in the region. The Beaufort, Chukchi, and East Siberian Seas, in particular, experience a greater range of cloud types and downwelling longwave radiation over offshore ice [*Eastman and Warren*, 2010]. Variation in cloud phase between supercooled water and ice may further affect the relationship between clouds and ice in these regions.

Biases in the reanalyses also contribute to the uncertainty in these results. For example, at high latitudes, ERA-Interim does not adequately simulate instances of thick clouds and large downwelling longwave fluxes during the winter [*Cox et al*., 2014]. Additionally, MERRA was found to have a downwelling longwave bias of $-12\,\mathrm{W\,m^{-2}}$ [*Cullather and Bosilovich*, 2012], which is 5–10% of the total downwelling longwave according to *Wang and Key* [2005a]. While the errors in the reanalyses must be acknowledged, the proper simulation of the winter cloud scene will provide an accurate surface flux at monthly time scales [*Walsh et al*., 2009], given the first-order relationship between cloud amount and the surface cloud radiative effect. Furthermore, the consistency in the relationship between wintertime cloud anomalies and summertime sea ice anomalies seen in the MODIS and MERRA products provides confidence that the relationship is real.

In the long term, the variability of sea ice cover may be related more to large-scale atmospheric circulation than local processes. *Ballinger and Rogers* [2014] examined the teleconnections between major atmospheric and oceanic indices and their effects on ice extent in the nearby Beaufort and Chukchi Seas, finding that the El Niño–Southern Oscillation (ENSO) has influenced ice extent retreat in recent years via the strongly positive Pacific/North American Pattern. Ice conditions in the East Siberian Sea were found to vary with high-index conditions of the Arctic Oscillation (AO) [*Rigor et al*., 2002].

However, a simple linear correlation analysis indicated that ENSO, AO, and Pacific Decadal Oscillation indices explained less than 10% of variance in both cloud cover and sea ice (individually) over the East Siberian Sea (not shown). It should be emphasized that none of the variances in cloud forcing or ice concentration anomaly explained by climate indices was greater than the variance in ice concentration explained by cloud cover anomalies.

6. Conclusions

Multiple climate processes are responsible for the recent decline in Arctic sea ice extent, including atmospheric heat and moisture advection, ocean circulation, freshwater input, and the ice-albedo feedback. These processes are described elsewhere [*Serreze et al*., 2007; *Francis et al*., 2009; *Stroeve et al*., 2012]. However, a consensus on

the interaction between clouds and sea ice extent has not been reached [*Kapsch et al.*, 2013; *Nussbaumer and Pinker*, 2012; *Graversen et al.*, 2011; *Kay et al.*, 2008; *Schweiger et al.*, 2008b; *Kauker et al.*, 2009].

The analysis presented here demonstrates that winter cloud cover anomalies can cause significant changes in summertime sea ice cover. As a case study, climate reanalysis data were used to show that the winter months preceding the 2007 sea ice minimum experienced cloud cover consistently above average in the East Siberian Sea. Results from MERRA, ERA-Interim, and remote sensing observations support this claim. This cloud anomaly translates into a theoretical decrease in sea ice thickness of 25 cm or greater than 40% of the ice thickness anomaly seen in 2007. Advecting the ice thickness anomalies with satellite-derived ice motion data resulted in a spatial pattern with striking similarities to the September ice concentration anomalies not only over the East Siberian and Kara Seas but also over a large region of the Arctic.

An examination of other years showed that the opposite relationship also occurs, i.e., that below-average winter cloud cover and surface cloud radiative forcing result in above-average summer sea ice cover. Furthermore, both of these relationships between winter cloud and summer sea ice were found to have occurred frequently over the last three decades, at least in the East Siberian and Kara Seas. Though many factors are related to sea ice growth and loss, the substantial variability in winter cloud cover clearly contributes to summer sea ice interannual variability. An examination of winter cloud cover can, therefore, be used to improve seasonal sea ice predictions.

Acknowledgments

This research was supported by the Joint Polar Satellite System (JPSS) Program Office and the NOAA Climate Data Records program. We are grateful to the University of Illinois Cryosphere Today website (http://arctic.atmos.uiuc.edu/cryosphere/) for providing their ice products to the scientific community. Sea ice data were obtained from the National Snow and Ice Data Center (NSIDC). MODIS data were acquired from the MODIS Adaptive Processing System (MODAPS) and can be downloaded at https://ladsweb.nascom.nasa.gov/data/search.html. CALIPSO data can be downloaded at https://eosweb.larc.nasa.gov/. MERRA data were downloaded from http://disc.sci.gsfc.nasa.gov/daac-bin/FTPSubset.pl?LOOKUPID_List=MAIMCPASM, and ERA can be found at http://apps.ecmwf.int/datasets/data/interim-full-mnth. We thank M. Tschudi for providing the sea ice motion data. The views, opinions, and findings contained in this report are those of the author(s) and should not be construed as an official National Oceanic and Atmospheric Administration or U.S. Government position, policy, or decision.

References

Ballinger, T. J., and J. C. Rogers (2014), Climatic and atmospheric teleconnection indices and western Arctic sea ice variability, *Phys. Geogr.*, *35*, 459–477.

Cavalieri, D. J., C. L. Parkinson, P. Gloersen, and H. Zwally (1996), Sea ice concentrations from Nimbus-7 SMMR and DMSP SSM/I-SSMIS passive microwave data Boulder, CO: NASA DAAC at the National Snow and Ice Data Center [2002–2013]. [Updated yearly.]

Cox, C. J., et al. (2014), Downwelling longwave flux over Summit, Greenland, 2010-2012: Analysis of surface-based observations and evaluation of ERA- Interim using wavelets, *J. Geophys. Res. Atmos.*, *119*, 12,317–12,337, doi:10.1002/2014JD021975.

Cullather, R. I., and M. G. Bosilovich (2012), The energy budget of the polar atmosphere in MERRA, *J. Clim.*, *25*, 5–24, doi:10.1175/2011JCLI4138.1.

Curry, J. A., W. B. Rossow, D. Randall, and J. L. Schramm (1996), Overview of Arctic cloud and radiation characteristics, *J. Clim.*, *9*, 1731–64.

Cuzzone, J., and S. Vavrus (2011), The relationships between Arctic sea ice and cloud-related variables in the ERA-Interim reanalysis and CCSM3, *Environ. Res. Lett.*, *6*, 014016.

Dee, D. P., et al. (2011), The ERA-Interim reanalysis: Configuration and performance of the data assimilation system, *Q. J. R. Meteorol. Soc.*, *137*, 553–97.

Deser, C., and H. Teng (2008), Evolution of Arctic sea ice concentration trends and the role of atmospheric circulation forcing, 1979–2007, *Geophys. Res. Lett.*, *35*, L02504, doi:10.1029/2007GL032023.

Eastman, R., and S. Warren (2010), Arctic cloud changes from surface and satellite observations, *J. Clim.*, *23*, 4233–4242.

Eisenman, I., N. Untersteiner, and J. S. Wettlaufer (2007), On the reliability of simulated Arctic sea ice in global climate models, *Geophys. Res. Lett.*, *34*, L10501, doi:10.1029/2007GL029914.

Fowler, C., W. Emery, and M. Tschudi (2013), *Polar Pathfinder Daily 25 km EASE-Grid Sea Ice Motion Vectors. Version 2*, National Snow and Ice Data Center, Boulder, Colo.

Francis, J. A., W. Chan, D. J. Leathers, J. R. Miller, and D. E. Veron (2009), Winter Northern Hemisphere weather patterns remember summer Arctic sea ice extent, *Geophys. Res. Lett.*, *36*, L07503, doi:10.1029/2009GL037274.

Graversen, R., T. Mauritsen, S. Drijfhout, M. Tjernström, and S. Mårtensson (2011), Warm winds from the Pacific caused extensive Arctic sea-ice melt in summer, 2007, *Clim. Dyn.*, *36*, 2103–12.

Holland, M. M., and C. M. Bitz (2003), Polar amplification of climate change in coupled models, *Clim. Dyn.*, *21*, 221–32.

Intrieri J. M., C. W. Fairall, M. D. Shupe, P. O. G. Persson, E. L. Andreas, P. S. Guest, and R. E. Moritz (2002), An annual cycle of Arctic surface cloud forcing at SHEBA, *J. Geophys. Res.*, *107*(C10), 8039, doi:10.1029/2000JC000439.

Kapsch, M. L., R. G. Graversen, and M. Tjernström (2013), Springtime atmospheric energy transport and the control of Arctic summer sea-ice extent, *Nat. Clim. Change*, *3*, 744–8.

Kauker, F., T. Kaminski, M. Karcher, R. Giering, R. Gerdes, and M. Voßbeck (2009), Adjoint analysis of the 2007 all time Arctic sea-ice minimum, *Geophys. Res. Lett.*, *36*, L03707, doi:10.1029/2008GL036323.

Kay, J. E., and A. Gettelman (2009), Cloud influence on and response to seasonal Arctic sea ice loss, *J. Geophys. Res.*, *114*, D18204, doi:10.1029/2009JD011773.

Kay, J. E., T. L'Ecuyer, A. Gettelman, G. Stephens, and C. O'Dell (2008), The contribution of cloud and radiation anomalies to the 2007 Arctic sea ice extent minimum, *Geophys. Res. Lett.*, *35*, L08503, doi:10.1029/2008GL033451.

Key, J., and X. Wang (2015), Climate Algorithm Theoretical Basis Document, Extended AVHRR Polar Pathfinder (APP-x) NOAA/NESDIS Center for Satellite Applications and Research and the National Climatic Data Center, Revision 1.0, September 2015, 85 pp.

Lindsay, R., M. Wensnahan, A. Schweiger, and J. Zhang (2014), Evaluation of seven different atmospheric reanalysis products in the Arctic, *J. Clim.*, *27*, 2588–2606.

Liu, Y., and J. R. Key (2014), Less winter cloud aids summer 2013 Arctic sea ice return from 2012 minimum, *Environ. Res. Lett.*, *9*, 044002, doi:10.1088/1748-9326/9/4/044002.

Liu, Y., J. Key, J. Francis, and X. Wang (2007), Possible causes of decreasing cloud cover in the Arctic winter 1982–2000, *Geophys. Res. Lett.*, *34*, L14705, doi:10.1029/2007GL030042.

Liu, Y., J. R. Key, and X. Wang (2008), The influence of changes in cloud cover on recent surface temperature trends in the Arctic, *J. Clim.*, *21*, 705–15.

Liu, Y., J. Key, and X. Wang (2009), Influence of changes in sea ice concentration and cloud cover on recent Arctic surface temperature trends, *Geophys. Research Lett.*, *36*, L20710, doi:10.1029/2009GL040708.
Liu, Y., J. R. Key, Z. Liu, X. Wang, and S. J. Vavrus (2012), A cloudier Arctic expected with diminishing sea ice, *Geophys. Res. Lett.*, *39*, L05705, doi:10.1029/2012GL051251.
Maslanik, J., and J. Stroeve (1999), Near-Real-Time DMSP SSM/I-SSMIS Daily Polar Gridded Sea Ice Concentrations, NASA DAAC at the National Snow and Ice Data Center, Boulder, Colo., [2002–2013]. [Updated daily.]
Nussbaumer, E. A., and R. T. Pinker (2012), The role of shortwave radiation in the 2007 Arctic sea ice anomaly, *Geophys. Res. Lett.*, *39*, L15808, doi:10.1029/2012GL052415.
Ogi, M., and I. G. Rigor (2013), Trends in Arctic sea ice and the role of atmospheric circulation, *Atmos. Sci. Lett.*, *14*, 97–101.
Overland, J. E., and M. Wang (2013), When will the summer Arctic be nearly sea ice free? *Geophys. Res. Lett.*, *40*, 2097–101, doi:10.1002/grl.50316.
Overland, J. E., J. A. Francis, E. Hanna, and M. Wang (2012), The recent shift in early summer Arctic atmospheric circulation, *Geophys. Res. Lett.*, *39*, L19804, doi:10.1029/2012GL053268.
Palm, S. P., S. T. Strey, J. Spinhirne, and T. Markus (2010), Influence of Arctic sea ice extent on polar cloud fraction and vertical structure and implications for regional climate, *J. Geophys. Res.*, *115*, D21209, doi:10.1029/2010JD013900.
Park, H.-S., S. Lee, Y. Kosaka, S.-W. Son, and S.-W. Kim (2015), The impact of Arctic winter infrared radiation on early summer sea ice, *J. Clim.*, doi:10.1175/JCLI-D-14-00773.1, in press.
Perovich, D. K., J. A. Richter-Menge, K. F. Jones, and B. Light (2008), Sunlight, water, and ice: Extreme Arctic sea ice melt during the summer of 2007, *Geophys. Res. Lett.*, *35*, L11501, doi:10.1029/2008GL034007.
Pithan, F., and T. Mauritsen (2013), Arctic amplification dominated by temperature feedbacks in contemporary climate models, *Nat. Geosci.*, *7*, 181–84.
Rienecker, M. M., et al. (2011), MERRA: NASA's Modern-Era Retrospective Analysis for Research and Applications, *J. Clim.*, *24*, 3624–48.
Rigor, I., J. Wallace, and R. Colony (2002), Response of sea ice to the Arctic Oscillation, *J. Clim.*, *15*, 2648–2663.
Schweiger, A. J. (2004), Changes in seasonal cloud cover over the Arctic seas from satellite and surface observations, *Geophys. Res. Lett.*, *31*, L12207, doi:10.1029/2004GL020067.
Schweiger, A., and J. R. Key (1994), Arctic Ocean radiative fluxes and cloud forcing estimates from the ISCCP C2 cloud dataset, *J. Appl. Meteorol.*, *33*, 948–63.
Schweiger, A. J., R. W. Lindsay, S. Vavrus, and J. A. Francis (2008a), Relationships between Arctic sea ice and clouds during autumn, *J. Clim.*, *21*, 4799–810.
Schweiger, A. J., J. Zhang, R. W. Lindsay, and M. Steele (2008b), Did unusually sunny skies help drive the record sea ice minimum of 2007? *Geophys. Res. Lett.*, *35*, L10503, doi:10.1029/2008GL033463.
Serreze, M. C., and J. A. Francis (2006), The Arctic amplification debate, *Clim. Change*, *76*, 241–64.
Serreze, M. C., M. M. Holland, and J. Stroeve (2007), Perspectives on the Arctic's shrinking sea-ice cover, *Science*, *315*, 1533–6.
Stone, R. S. (1997), Variations in western Arctic temperature in response to cloud radiative and synoptic-scale influences, *J. Geophys. Res.*, *102*, 21,769–76.
Stone, R. S., D. Douglas, G. Belchansky, and S. Drobot (2005), Correlated declines in Pacific Arctic snow and sea ice cover, *Arctic Res. United States*, *19*, 18–25.
Stroeve, J. C., M. C. Serrez, M. M. Holland, J. E. Kay, J. Maslanik, and A. P. Barrett (2012), The Arctic's rapidly shrinking sea ice cover: A research synthesis, *Clim. Change*, *110*, 1005–27.
Thorndike, A. S. (1992), A toy model linking atmospheric thermal radiation and sea ice growth, *J. Geophys. Res.*, *97*, 9401–10.
Tjernström, M., J. Sedlar, and M. D. Shupe (2008), How well do regional climate models reproduce radiation and clouds in the Arctic? An evaluation of ARCMIP simulations, *J. Appl. Meteorol. Climatol.*, *47*, 2405–22.
Vavrus, S., D. Waliser, A. Schweiger, and J. Francis (2009), Simulations of 20th and 21st century Arctic cloud amount in the global climate models assessed in the IPCC AR4, *Clim. Dyn.*, *33*, 1099–115.
Vavrus, S., M. M. Holland, and D. A. Bailey (2011), Changes in Arctic clouds during intervals of rapid sea ice loss, *Clim. Dyn.*, *36*, 1475–89.
Walsh, J. E., W. L. Chapman, and D. H. Portis (2009), Arctic cloud fraction and radiative fluxes in atmospheric reanalyses, *J. Clim.*, *22*, 2316–2334.
Wang, J., J. Zhang, E. Watanabe, M. Ikeda, K. Mizobata, J. E. Walsh, X. Bai, and B. Wu (2009), Is the Dipole Anomaly a major driver to record lows in Arctic summer sea ice extent? *Geophys. Res. Lett.*, *36*, L05706, doi:10.1029/2008GL036706.
Wang, X. J., and J. R. Key (2003), Recent trends in arctic surface, cloud, and radiation properties from space, *Science*, *299*, 1725–8.
Wang, X., and J. Key (2005a), Arctic surface, cloud, and radiation properties based on the AVHRR Polar Pathfinder data set. Part I: Spatial and temporal characteristics, *J. Clim.*, *18*(14), 2558–2574.
Wang, X. J., and J. R. Key (2005b), Arctic surface, cloud, and radiation properties based on the AVHRR Polar Pathfinder dataset. Part II: Recent trends, *J. Clim.*, *18*, 2575–93.
Wang, X., J. Key, and Y. Liu (2010), A thermodynamic model for estimating sea and lake ice thickness with optical satellite data, *J. Geophys. Res.*, *115*, C12035, doi:10.1029/2009JC005857.
Winker, D. M., J. Pelon, and M. P. McCormick (2003), The CALIPSO mission: Spaceborne lidar for observation of aerosols and clouds, Proc, *SPIE 4893*, 1–11.
Zhang, X., and J. E. Walsh (2006), Toward a seasonally ice-covered Arctic Ocean: Scenarios from the IPCC AR4 model simulations, *J. Clim.*, *19*, 1730–47.
Zib, B. J., X. Dong, B. Xi, and A. Kennedy (2012), Evaluation and intercomparison of cloud fraction and radiative fluxes over the Arctic using BSRN surface observations, *J. Clim.*, *25*, 2291–2305, doi:10.1175/JCLI-D-11-00147.1.